EFFECT OF TRAFFIC INTERRUPTION PROBABILITY IN CAR-FOLLOWING MODEL WITH ELECTRONIC THROTTLE UNDER CONNECTED ENVIRONMENT

Abstract

As the number of vehicles increases, traffic interruption phenomena become more frequent. In order to better understand and control traffic flow, we proposed a car-following model in this work by taking into account the effect of traffic interruption probability with electronic throttle angle under a connected vehicle environment called the IP-ET model. The linear stability theory is employed to establish the stability condition of the proposed model. The stability curve demonstrated that by considering the effect of interruption probability with throttle angle leads to an enhancement in the region of traffic flow stability when compared to existing models. Through nonlinear analysis, the study derived the mKdV equation, which effectively describes the propagation of traffic flow density waves in proximity to the critical point. Furthermore, the numerical findings align with the theoretical results, affirming the validity of the proposed model and observing that the IP-ET model effectively enhances the efficiency of vehicle movement, reduces traffic congestion, and contributes to overall road safety.

Keywords: Traffic interruption probability, Throttle angle, Car-following, Stability analysis.

Authors

Sunita Yadav
Department of Mathematics
Maharshi Dayanand University
Rohtak, Haryana, India.
sunita.rs.maths@mdurohtak.ac.in

Poonam Redhu
Department of Mathematics
Maharshi Dayanand University
Rohtak, Haryana, India.
poonamr.maths@mdurohtak.ac.in

I. INTRODUCTION

As communication and information technologies provide major benefits for transportation, security, and environmental sustainability, connected and autonomous vehicles (CAVs) have attracted a lot of interest recently in both business and academia [1, 2, 3]. In a CAV system, vehicle-to-vehicle (V2V) communication is a crucial aspect that facilitates collaboration among individual vehicles on the road. For instance, in order to prevent crashes in an automated traffic stream, it is preferable for vehicles to communicate information about one another using V2V communications [4].

Traffic flow models are essential for transportation planners, engineers, and policymakers to analyze and improve traffic management, design efficient road networks, and optimize transportation systems. Generally, traffic flow modells can be categorized into two groups: microscopic and macroscopic models. Microscopic traffic flow models [5, 6] focus on capturing the behavior of individual vehicles and their interactions at a granular level, typically using microscopic variables such as velocity, position, and acceleration. On the other hand, macroscopic traffic flow models [7, 8] take a more aggregated approach, describing traffic flow using macroscopic variables that provide an overview of traffic conditions on a larger scale. These variables include traffic density, flow rate and average speed of the traffic stream. Microscopic traffic flow models can be further classified into different subcategories, with car-following (CF) models and cellular automaton (CA) models being two common approaches. Car-following (CF) models describe the behavior of individual vehicles while following the lead of preceding cars in an identical path, rely on the concept that every motorist manages their car by responding to stimuli from the car directly ahead. Car-following models encompass a range of approaches, such as the GHR model [9] and its modifications [10, 11, 12], the Gipps model [13], the optimal velocity (OV) model [14], intelligent driver model [15], fuzzy-logic model [16] and deep learning neural network [17]. Bando et al. developed an OV model [14] which states that the following vehicle aims to maintain a secure speed based on the difference between the current vehicle and the one ahead in traffic flow. Since then, several variations of the OV-based CF models come into existence by considering the surrounding conditions of the subsequent car in a traffic stream [18, 19, 20, 21, and 22]. Li et al. [[23]] introduced a CF model that considers the influence of the "electronic throttle opening angle" of the leading vehicle that is closest, building upon the FVD model [19]. Their study revealed improved traffic flow stability as compared to the FVDM. Subsequently, in 2017, they extended their model to incorporate both the sideways distance between vehicles and "electronic throttle opening angle" effects under connected environments [24]. However, these two models only accounted for the "electronic throttle opening angle" of the closest preceding vehicle, failing to capture the characteristics of the internet of vehicles in CAVs. To address this limitation, Qin et al. [25] introduced a CAV car-following model that incorporates the impact of feedback regulate of "electronic throttle opening angles" for numerous leading cars. Sun et al. [26] investigate the same effect of the on a curved road. Furthermore, many existing research [27, 28, 29, 30] has provided evidence that the dynamics of electronic throttle can impact the flow of traffic.

As we know, frequent occurrences of traffic accidents can result in disruptions to the flow of traffic. To understand the underlying factors influencing traffic interruptions, several traffic models have been developed, taking different accidents into account [31, 32, and 33]. A macro model [34] was introduced, incorporating an interrupt probability parameter.

Furthermore, a two-lane macro model [35] was established, considering traffic interruption probability based on the Ref. [34]. Notably, Tang et al. [36] proposed a CF model that considers the probability of traffic interruptions and Peng [37] incorporates the anticipation term related to traffic interruptions. It's important to note that in real traffic scenarios, traffic interruptions can be unpredictable. In reality, certain traffic interruptions occur with certain probabilities and give rise to complex phenomena within the traffic flow.

Thus, in this study, we improve existing traffic models by incorporating traffic interruption probability and electronic throttle dynamics, which were not considered in previous models. The motivation behind this study is to better understand the impact of interruptions, such as accidents, pedestrians, tolling stations, and signal lights, on CAV traffic flow. In particular, a new CF model is developed that incorporates the impact of traffic interruptions and electronic throttle angle within a connected environment. Thus, the proposed model plays a crucial role in the CAV environment which allows us to evaluate the effectiveness of CAV traffic flow with regards to its consistency, stability, and important metrics like distance headway, speed, and acceleration/deceleration characteristics. By incorporating these elements, we can better understand and optimize the overall efficiency of CAV traffic flow.

The following is a description of the paper's structure. In Section II, we review the basic models and introduce the IP-ET model. Linear and nonlinear stability analysis is examined in Sections III and IV, respectively. Section V carried out numerical simulation and finally, the conclusion is provided in Section VI.

II. MODEL

Bando et al. [14] proposed the OV model, which revolves around the concept that drivers aim to adjust their speed to attain an optimal speed. The model is represented by the following equation:

$$\frac{dv_j(\tilde{t})}{d\tilde{t}} = a\left(V\left(s_j(\tilde{t})\right) - v_j(\tilde{t})\right) \tag{1}$$

where a denotes the driver's sensitivity coefficient, x_j and v_j denote the position and speed of the vehicle j, respectively, $s_j = x_{j+1} - x_j$ denotes the headway between the vehicle j and the vehicle $j + 1$, and $V(s_j)$ denotes the optimal velocity function as defined by

$$V\left(s_j(\tilde{t})\right) = \frac{v_{max}}{2}\left[tanh\left(s_j(\tilde{t}) - h_c\right) + tanh(h_c)\right] \tag{2}$$

where h_c denotes the proper separation and v_{max} signifies the maximum speed achievable by the vehicle. The primary drawback of the OV model was its tendency to exhibit rapid acceleration rates and unlikely deceleration patterns. To address these limitations, Jiang et al. [19] proposed the "full velocity difference (FVD) model" by incorporating positive velocity differences into the OV model as

$$\frac{dv_j(\tilde{t})}{d\tilde{t}} = a\left(V\left(s_j(\tilde{t})\right) - v_j(\tilde{t})\right) + \lambda\Delta v_j(\tilde{t}) \tag{3}$$

where $\Delta v_j(\tilde{t}) = v_{j+1}(\tilde{t}) - v_j(\tilde{t})$ represent the relative speed between the jth and $j+1^{th}$ vehicles and λ is the sensitivity coefficient of relative speed.

Li et al. [[23]] introduced a model called the throttle-based FVD (T-FVD) by combining the electronic throttle opening angle of CAVs with the FVD model which is expressed as

$$\frac{dv_j(\tilde{t})}{d\tilde{t}} = a\left(V\left(s_j(\tilde{t})\right) - v_j(\tilde{t})\right) + \lambda \Delta v_j(\tilde{t}) + \kappa\left(\Delta\theta_j(\tilde{t})\right) \tag{4}$$

Where $\Delta\theta_j = \theta_{j+1}(\tilde{t}) - \theta_j(\tilde{t})$ are the electronic throttle opening angles of the $(j+1)^{th}$ vehicle and following vehicle j^{th}, κ represents the control coefficient that governs the angle difference. By manipulating the electronic throttle (ET) angle, drivers have the ability to alter the velocity of their vehicles. This can be achieved by understanding and applying the dynamic equation associated with the ET angle. By taking into account factors such as the vehicle's velocity and acceleration, drivers are able to effectively control and adjust their speed as desired, which is expressed as

$$a_j(\tilde{t}) = -c(v_j(\tilde{t}) - v_e) + d(\theta_j(\tilde{t}) - \theta_e) \tag{5}$$

Where $c > 0$, $d > 0$ are coefficients, the steady-state velocity of the automobile is represented by v_e, θ_e denotes the steady-state ET angle corresponding to the velocity v_e, $a_j(\tilde{t})$ is the acceleration of the jth vehicle. The opening angle of the ET denoted by $\Delta\theta_j(\tilde{t})$, is determined using Eq. (5) as follows:

$$\Delta\theta_j(\tilde{t}) = \frac{1}{d}\left(\Delta a_j(\tilde{t}) + c\,\Delta v_j(\tilde{t})\right) \tag{6}$$

While the car-following models mentioned above are effective in describing complex traffic patterns, however, they may not directly address phenomena caused by traffic interruptions such as accidents, pedestrians, tolling stations, signal lights, etc. These factors introduce unique dynamics and complexities that require separate study and analysis. Indeed, there is a possibility of interruptions occurring in each vehicle. Considering the analysis mentioned above, we proposed a model by considering the effect of traffic interruption probability (IP) with electronic throttle (ET) angle under a connected vehicle environment, called the IP-ET model. The control equation for the proposed model is as follows:

$$\begin{aligned}\frac{dv_j(\tilde{t})}{d\tilde{t}} = a\left(V\left(s_j(\tilde{t})\right) - v_j(\tilde{t})\right) &+ \lambda_1\,p_{j+1}(-v_j) + \lambda_2(1 - p_{j+1})\Delta v_j(\tilde{t}) \\ &+ \kappa\,\Delta\theta_j(\tilde{t})\end{aligned} \tag{7}$$

Where p_{j+1} representing the probability of the preceding car being interrupted and λ_1, λ_2 are the response factors. When the preceding car is entirely interrupted, its velocity instantaneously drops to zero, resulting in a velocity difference of $(-v_j)$ between the $(j+1)^{th}$ and the jth cars.

The traffic IP is influenced by traffic conditions and road layout. For simplicity, we assumes that the IP p_{j+1} is constant, denoted as p. We discretize Eq. (7) using the asymmetric forward difference as follows to do stability analysis:

$$s_j(\tilde{t} + 2\tau) = s_j(\tilde{t} + \tau) + \tau\big[V(s_{j+1}(\tilde{t})) - V(s_j(\tilde{t}))\big] + \lambda_1 p\big(-s_j(\tilde{t}+\tau) + s_j(\tilde{t})\big) +$$
$$\lambda_2(1-p)\big(s_{j+1}(\tilde{t}+\tau) - s_{j+1}(\tilde{t}) - s_j(\tilde{t}+\tau) + s_j(\tilde{t})\big) + \frac{\kappa c \tau}{d}\big(s_{j+1}(\tilde{t}+\tau) - s_{j+1}(\tilde{t}) -$$
sjt+τ+sjt+κ   dsj+1t+2τ− 2sj+1t+τ+sj+1t− sjt+2τ+2sjt+τ− sjt
(8)

III. LINEAR STABILITY ANALYSIS

We conduct the linear stability analysis using the perturbation approach to determine the stability condition of the proposed (IP-ET) model. We assume that all cars are traveling at the optimal speed $V(h)$ and maintaining a consistent distance of h between them.
A stable state requires the following conditions:

$$x_j^0(\tilde{t}) = hj + V(h)\tilde{t}, h = \frac{L}{N} \qquad (9)$$

where N and L represent the number of cars and the length of the route, respectively. In the traffic steady state $x_j^0(\tilde{t})$, we introduce a small deviation $y_j(\tilde{t})$ which is given below

$$x_j(\tilde{t}) = x_j^0(\tilde{t}) + y_j(\tilde{t}) \qquad (10)$$

The headway is represented as $s_j(\tilde{t}) = h + \Delta y_j(\tilde{t})$. By substituting these values into Eq. (8) linearizing the equation, and ignoring the nonlinear terms, we derive the following result:

$$\Delta y_j(\tilde{t} + 2\tau) = \Delta y_j(\tilde{t} + \tau) + \tau V'(h)\big(\Delta y_{j+1}(\tilde{t}) - \Delta y_j(\tilde{t})\big)$$
$$+ \lambda_1 p\big(-\Delta y_j(\tilde{t}+\tau) + \Delta y_j(\tilde{t})\big)$$
$$+ \lambda_2(1-p)\big(\Delta y_{j+1}(\tilde{t}+\tau) - \Delta y_{j+1}(\tilde{t}) - \Delta y_j(\tilde{t}+\tau) + \Delta y_j(\tilde{t})\big)$$
$$+ \frac{\kappa c \tau}{d}\big(\Delta y_{j+1}(\tilde{t}+\tau) - \Delta y_{j+1}(\tilde{t}) - \Delta y_j(\tilde{t}+\tau) + \Delta y_j(\tilde{t})\big)$$
$$+ \frac{\kappa}{d}\big(\Delta y_{j+1}(\tilde{t}+2\tau) - 2\Delta y_{j+1}(\tilde{t}+\tau) + \Delta y_{j+1}(\tilde{t}) - \Delta y_j(\tilde{t}+2\tau)$$
$$+ 2\Delta y_j(\tilde{t}+\tau) - \Delta y_j(\tilde{t})\big) \qquad (11)$$

By expanding $\Delta y_j(\tilde{t}) = Ae^{ijk+z\tilde{t}}$ in equation (11) using Fourier series and then substituting $z = z_1(ik) + z_2(ik)^2 + \ldots$ and $e^{ik} = 1 + ik + \frac{1}{2} + \ldots$, while neglecting terms of order greater than the second order, we obtain

$$[z_1(ik) + z_2(ik)^2]\tau + \frac{3}{2}z_1^2(ik)^2\tau^2 = \tau\, V'(h)\left((ik) + \frac{(ik)^2}{2}\right) - \lambda_1 p\left[(z_1(ik) + \right.$$

z2ik2τ   +z12ik2τ22   +   λ21−   pτ   z1ik2+κ   cdτ2z1ik2
(12)

By equating the first and second-order components of ik, we get

$$z_1 = \frac{V'(h)}{1+\lambda_1\, p} \tag{13}$$

$$z_2 = \frac{V'(h)-z_1^2\tau(3+\lambda_1 p)+2\lambda_2\,(1-p)z_1+\frac{2\kappa\, c}{d}z_1\tau}{1+\lambda_1\, p} \tag{14}$$

According to stability theory, the model will be in a stable state when criteria $z_1 > 0$ and $z_2 > 0$ are satisfied. The stability condition is as a result

$$a > \frac{(3+\lambda_1 p)V'(h)-\frac{2\kappa\, c}{d}(1+\lambda_1\, p)}{(1+\lambda_1\, p)^2+2(1+\lambda_1 p)\lambda_2(1-p)} \tag{15}$$

When $p = 0$ the neutral stability curve remains identical to that of the T-FVD model [23] and the proposed IP-ET model is deduced to the FVD model [19] for $\kappa = 0$ and $p = 0$. Additionally, if the parameters satisfy the conditions $\kappa = 0$, $\lambda_2 = 0$, and $p = 0$, the proposed IP-ET model reduces to the OV model [14], and its stability condition becomes the same as that of the OV model [14]. Thus, the findings validate the efficiency of the suggested model and the accuracy of the stability analysis.
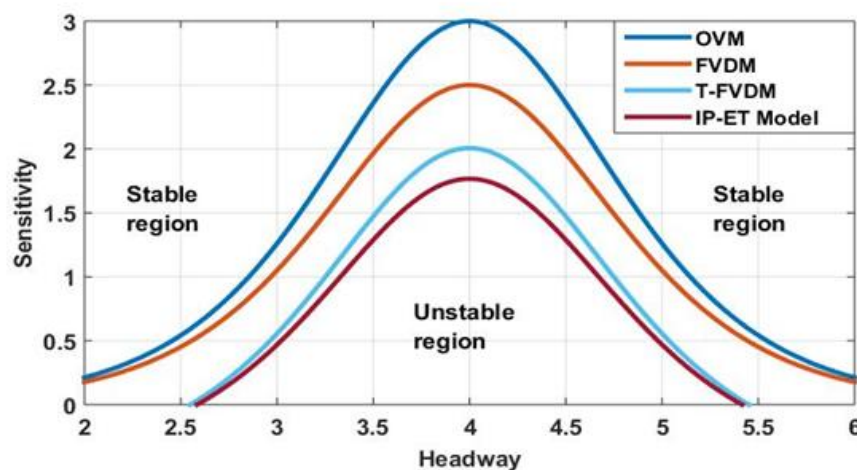

Figure 1: Comparison of Phase Diagram between the OVM, FVDM, T-FVDM and Proposed IP-ET Model.

Figure 1 illustrates a comparison between different traffic flow models (OV model, FVD model, T-FVD model) along with a proposed model for fixed value of parameters $p = 0.2$ and $\kappa = 0.1$. The critical curve in Fig. 1 separates the space formed by the sensitivity coefficient and the space headway into two regions: the stable region and the

unstable region. The stable region represents traffic flow conditions where the flow remains stable, while the unstable region shows the emergence of density waves, indicating unstable traffic flow conditions. Figure 1 illustrates that under the identical value of h_c (headway), the value of sensitivity coefficient (a_c) at the critical point obtained from the IP-ET model is the lowest among all the existing models (OV model, FVD model, and T-FVD model). This suggests that the proposed model exhibits better stability characteristics as compared to the other models.

Figure 2(a) shows the phase diagram of the IP-ET model for various values interruption probability p with fixed $\lambda_1 = 0.5$, $\lambda_2 = 0.1$ and control coefficient of electronic throttle dynamics $\kappa = 0.1$.

It is clearly seen from Figure 2(a) that the stable region expands as the value of the traffic interruption probability (p) rises. Also, the lowering of the amplitude and critical point of the stability curves indicate that the traffic flow system becomes stronger and less sensitive to variations in the traffic interruption probability. This suggests that when drivers are more aware of potential traffic interruptions and adjust their driving behavior accordingly, the overall stability of traffic flow improves.
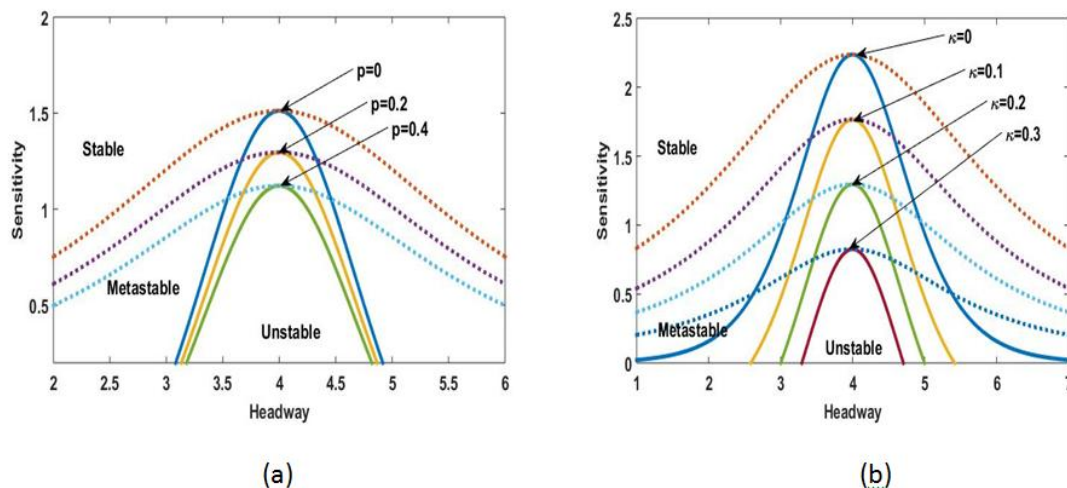

Figure 2: Phase Diagram in Headway-Sensitivity for Various values of (a) Traffic Interruption Probability (IP) p and (b) Electronic Throttle Angle (ET) κ

The phase diagram of the IP-ET model is shown in Fig. 2(b) for different values of $\kappa = 0, 0.1, 0.2, 0.3$ for a fixed interruption probability $p = 0.2$. With an increase in the value of κ, the stable zone expands progressively while the neutral and coexistence stability curves drastically degrade. It implies that by assuming the dynamics of the ET opening angle, the system's overall stability is enhanced. It means that accounting for the electronic throttle's behavior allows for better control and regulation of the system, resulting in a more stable and reliable operation.

Thus, the relevant parameters play a crucial role in the stability of traffic flow, therefore the IP-ET model that consider the driver's traffic interruption probability with

electronic throttle effects under a connected vehicle environment are effectively suppresses traffic congestion.

IV. NONLINEAR ANALYSIS

In order to further investigate the impacts of the traffic IP and ET on the stability of traffic flow, we carry out a nonlinear analysis of the slowly varying behavior of long waves in stable and unstable zones. We define slow variables X and T and introduce the slow scales for space variable j and time variable $\tilde{t}$.

$$X = \epsilon(j + b\tilde{t}), T = \epsilon^3 \tilde{t}, 0 < \epsilon \leq 1 \tag{16}$$

where b is the unspecified constant.

The distance between vehicles $s_j(\tilde{t})$ is given as

$$s_j = h_c + \epsilon R(X, T) \tag{17}$$

Using Eqs. (16) and (17) into Eq. (8), the following nonlinear evolution problem is obtained by expanding using Taylor's series expansion up to the fifth power of ϵ

$$\epsilon^2 m_1 \partial_X R + \epsilon^3 m_2 \partial_X^2 R + \epsilon^4 [m_3 \partial_X^3 R + m_4 \partial_X R^3 + (1 + \lambda_1 p)\partial_T R]$$
$$+ \epsilon^5 [m_5 \partial_X^4 R + m_6 \partial_X^2 R^3 + m_7 \partial_X \partial_T R] = 0 \tag{18}$$

where

$$m_1 = b(1 + \lambda_1 p) - V'(h)$$
$$m_2 = \frac{b^2 \tau}{2}(3 + \lambda_1 p) - \frac{V'(h)}{2} - \lambda_2(1 - p)b - \frac{\kappa c}{d} b \tau$$
$$m_3 = \frac{b^3 \tau^2}{6}(7 + \lambda_1 p) - \frac{V'(h)}{6} - \left(\lambda_2(1 - p) + \frac{\kappa c \tau}{d}\right)\frac{(b^2 \tau + b)}{2} - \frac{\kappa}{d} b^2$$
$$m_4 = -\frac{V'''(h)}{6}$$

$$m_5 = \frac{b^4 \tau^3}{24}(15 + \lambda_1 p) - \frac{V'(h)}{24} - \left(\lambda_2(1 - p) + \frac{\kappa c \tau}{d}\right)\frac{(4b^3 \tau^3 + 6b^2 \tau + 4b)}{24}$$
$$- \frac{\kappa}{d}\left(b^3 \tau^2 + \frac{b^2 \tau}{2}\right)$$
$$m_6 = -\frac{V'''(h)}{12}$$
$$m_7 = \left(b\tau(3 + \lambda_1 p) - \lambda_2(1 - p) - \frac{\kappa c \tau}{d}\right)$$

And

$$V'(h) = \frac{dV(s_j)}{ds_j}\Big| s_j = h, V'''(h) = \frac{d^3 V(s_j)}{ds_j^3}\Big| s_j = h$$

By considering traffic flow near the critical point $a_c/a = (1 + \epsilon^2)$, $a_c = \frac{(3+\lambda_1 p)V'(h_c)-\frac{2\kappa c}{d}(1+\lambda_1 p)}{(1+\lambda_1 p)^2+2(1+\lambda_1 p)\lambda_2(1-p)}$ and taking

$b = \frac{V'(h_c)}{1+\lambda_1 p}$ into Eq. (18), we obtained the following equation after neglecting the terms of second and third orders of ϵ as

$$\epsilon^3(\partial_T R - q_1\partial_X^3 R + q_2\partial_X R^3) + \epsilon^5(q_3\partial_X^2 R + q_4\partial_X^4 R + q_5\partial_X^2 R^3) = 0 \tag{19}$$

where

$$q_1 = \frac{b^3\tau_c^2}{6}(7 + \lambda_1 p) - \frac{V'(h_c)}{6} - \left(\lambda_2(1-p) + \frac{\kappa c\tau_c}{d}\right)\frac{(b^2\tau_c+b)}{2} - \frac{\kappa}{d}b^2\tau_c$$

$$q_2 = -\frac{V'''(h_c)}{6}$$

$$q_3 = \frac{b^2\tau_c}{2}(1 + \lambda_1 p) + \frac{\kappa c\tau_c}{d},$$

$$q_4 = \frac{b^4\tau_c^3}{24}(15 + \lambda_1 p) - \frac{V'(h_c)}{24} - \left(\lambda_2(1-p) + \frac{\kappa c\tau_c}{d}\right)\frac{(4b^3\tau_c^3+6b^2\tau_c+4b)}{24} - $$

$$\frac{\kappa}{d}\left(b^3\tau_c^2 + \frac{b^2\tau_c}{2}\right) - \left((3 + \lambda_1 p)b\tau_c - \lambda_2(1-p) + \frac{\kappa c\tau_c}{d}\right)\frac{q_1}{(1+\lambda_1 p)}$$

$$q_5 = -\frac{V'''(h_c)}{12} + \left((3 + \lambda_1 p)b\tau_c - \lambda_2(1-p) + \frac{\kappa c\tau_c}{d}\right)\frac{V'''(h_c)}{6(1+\lambda_1 p)}$$

The following transformation (Change of scale variable) is applied to Eq. (19) to obtain the mKdV equation

$$\tilde{T} = \frac{1}{q_1}T, \tilde{R} = \sqrt{\frac{q_1}{q_2}}R \tag{20}$$

Therefore, the conventional mKdV equation is provided with such a $O(\epsilon)$ correction term

$$\partial_{\tilde{T}}\tilde{R} = \partial_X^3\tilde{R} - \partial_X\tilde{R}^3 - \epsilon\left(\frac{q_3}{q_1}\partial_X^2\tilde{R} + \frac{q_4}{q_1}\partial_X^4\tilde{R} + \frac{q_5}{q_1}\partial_X^2\tilde{R}^3\right) \tag{21}$$

If the term $O(\epsilon)$ is neglected, the "kink-antikink" soliton is defined as

$$\tilde{R}_0(X, \tilde{T}) = \sqrt{c} \sim \tanh\sqrt{\frac{c}{2}}(X - c\tilde{T}) \tag{22}$$

By using $\tilde{R}_0(X, \tilde{T})$ and determining propagation velocity u, the kink solution must fulfill the solvability criteria

$$\left(\tilde{R}_0, M[\tilde{R}_0]\right) \equiv \int_{-\infty}^{\infty}\tilde{R}_0 M[\tilde{R}_0]dX = 0 \tag{23}$$

where $M[\tilde{R}_0] = \left(\frac{q_3}{q_1}\partial_X^2\tilde{R} + \frac{q_4}{q_1}\partial_X^4\tilde{R} + \frac{q_5}{q_1}\partial_X^2\tilde{R}^3\right).$

We determine propagation velocity u as a result of the method mentioned in Ref. [[38]]:

$$u = \frac{5q_2q_3}{2q_2q_4 - 3q_1q_5} \tag{24}$$

As a result, the following is the general kink-antikink solution:

$$s_j(\tilde{t}) = h_c \pm \sqrt{\frac{q_1 u}{q_2}\left(\frac{\tau}{\tau_c} - 1\right)} \times \left[\left(1 - u\, q_1\right)\left(\frac{\tau}{\tau_c} - 1\right)\tilde{t} + j\right] \tag{25}$$

The amplitude is

$$\tilde{A} = \sqrt{\frac{q_1 u}{q_2}\left(\frac{\tau}{\tau_c} - 1\right)} \tag{26}$$

The presence of both jammed and free flow phases, characterized by $s_j = h_c \pm \tilde{A}$, demonstrate the coexistence of curves. Consequently, the jamming transition can be effectively defined using the mKdV equation. In the parameter space (h_c, a_c), Fig. 2 illustrates the replication of neutral stability curves (solid lines) with coexisting curves (dotted lines) through nonlinear analysis.

These curves correspond to the two coexisting phases: the freely flowing phase at low density and the congested jam at high density, which are represented by the "kink-antikink" solution. The nonlinear analysis suggests that the solution of the mKdV equation, near the critical point, effectively represents the propagating characteristic of traffic jams.

V. NUMERICAL SIMULATION

In this section, numerical simulations are carried out with periodic boundary conditions using Eq. (8). To study the spatial-time development of the headway, a small disturbance will be introduced to the uniform flow. The initial conditions for the study are as follows:

$$s_j(0) = s_j(1) = s_j(2) = 4.0, \quad (j \neq 50,51)$$

$$s_j(0) = s_j(1) = s_j(2) = 4.0 + A, \quad (j = 50)$$

$$s_j(0) = s_j(1) = s_j(2) = 4.0 - A, \quad (j = 51)$$

Other factors are set as $\lambda_1 = 0.5, \lambda_2 = 0.1, c = 0.8, d = 0.27$ and $a = 1.6$. When time $\tilde{t} = 10,300$, the headway profiles correspond to the Figs. 2(a) and 2(b) are displayed in Figs. 3(a) and 3(b) respectively.
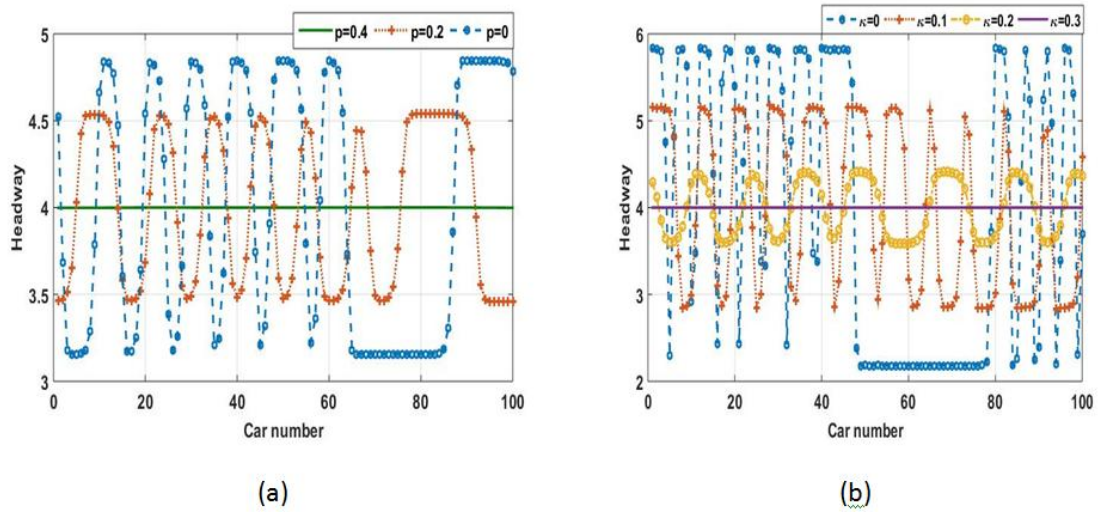
Figure 3: Headway Evolution for Different values of (a) Traffic Interruption Probability (IP) p with fixed ET $\kappa = 0.1$ (b) Electronic Throttle Angle (ET) κ with Fixed IP $p = 0.2$

Figures 3(a) show that when a small perturbation is introduced to the conventional traffic flow, stop-and-go traffic congestion appears in the unstable region and expands downstream with time. As the value p increases, the amplitude as well as the number of kink-antikink waves, decreases and if we enter into the stable region, the perturbation dies out which leads to uniform flow.
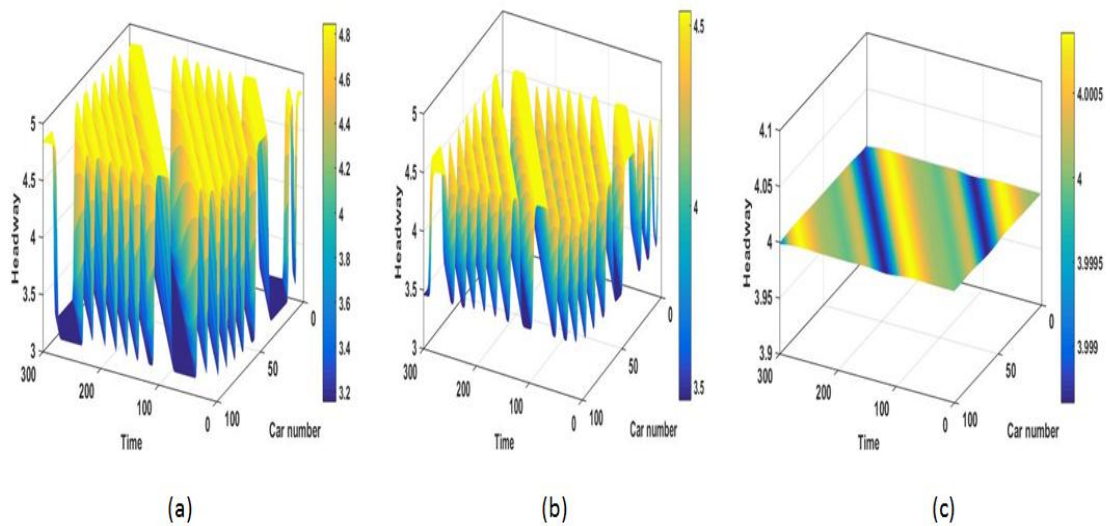

Figure 4: Headway Evolution for Different Values of p (a) $p = 0$ (b) $p = 0.2$ (c) $p = 0.4$ with Fixed ET $\kappa = 0.1$

Figure 4 represents spatial-temporal evolution of the headway corresponding to Fig. 3(a) for $\kappa = 0.1$. As seen in Figs. 4(a)-(b), the initial perturbation develops into congested flow in the form of kink waves that go backward and fluctuate close to the critical headway. As we reach into the stable region for $p = 0.4$, it is obvious from Fig. 4(c) that the congested flow converts into the uniform flow. Moreover, we can say that when the parameters set

satisfies the stability criterion (15) the amplitude of stop-and-go waves dies out, representing a state of uniform flow and the traffic flow will continue in the stable state even in the presence of a small perturbation. Hence, to improve the stability of traffic flow, it is crucial to incorporate the traffic interruption probability into the CF model.

Figure 3(b) displays the headway profile for various values of κ, for fixed $p = 0.2$ at $\tilde{t} = 10300$ in respective of Fig. 2(b) which indicates that the amplitude of headway profile diminishes with increase in values of κ and flow become uniform for $\kappa = 0.3$. Figure 5 depicts spatial-temporal evolution of the headway with different parameter κ in respect to Fig. 3(b) with fixed IP parameter value $p = 0.2$. The initial perturbation evolves into a "kink-antikink" wave, which oscillates near the critical headway as shown in Figs. 5(a)-(c) the number of stop-and-go waves, as well as their amplitude, decreases with the increment in the value of κ which is remarkably similar to the solution of the mKdV equation because the stability criterion (15) does not satisfy. Figure 5(d) shows that once we approach in the stable zone for $\kappa = 0.3$ the congested flow transforms into a uniform flow. The smoothness and stability of traffic flow are thereby improved by including electronic throttle (ET) dynamics in the model.
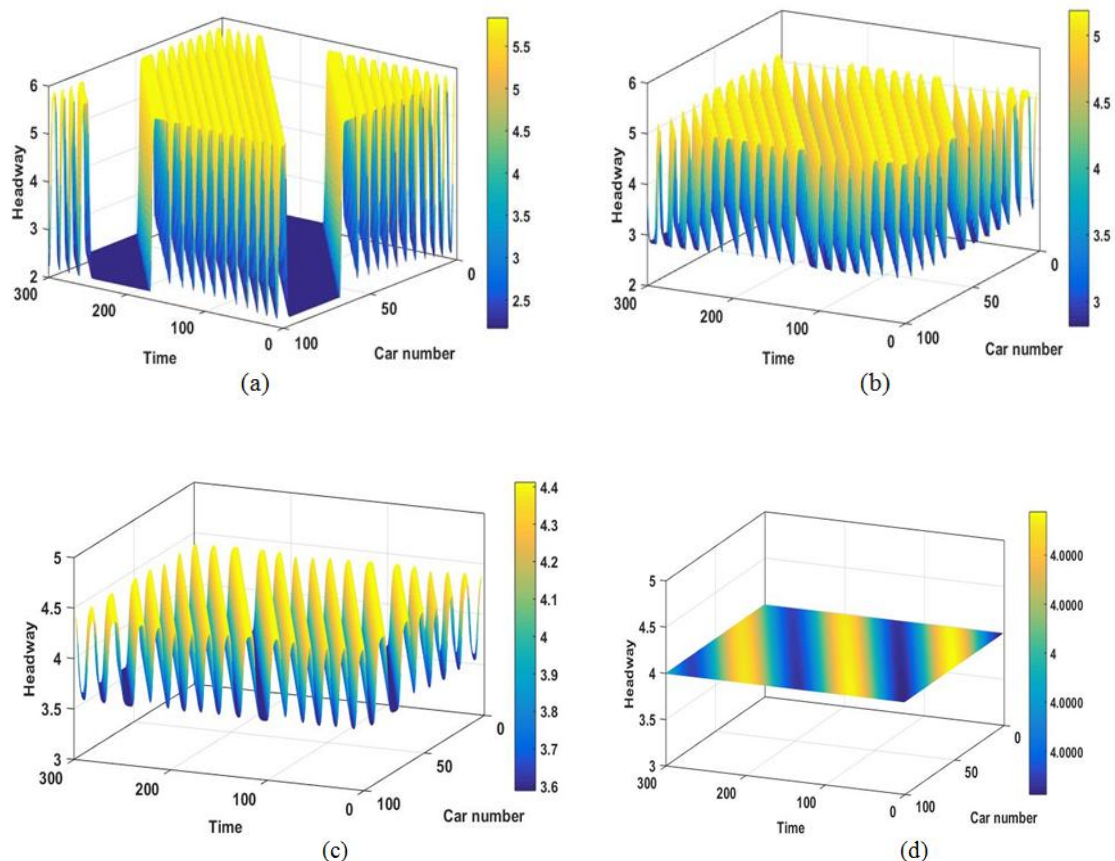

Figure 5: Headway Evolution for Different values of κ with Fixed Interruption Probability $p = 0.2$ (a) $\kappa = 0$ (b) $\kappa = 0.1$ (c) $\kappa = 0.2$ (d) $\kappa = 0.3$

Thus, under connected vehicles, the stability of traffic flow is enhanced by taking into account the traffic interruption probability with electronic throttle dynamics. As a result, the simulation findings are in accordance with the theoretical study.

VI. CONCULSION

The increasing complexity of the modern traffic environment has led to a rise in the frequency of traffic interruptions. Due to the frequent occurrence of traffic interruptions, it is crucial to address this issue in traffic modeling and car-following models. In this study, we developed a car-following model named the IP-ET model by considering the effect of traffic interruption probability with throttle angle under a connected vehicle environment, aiming to better understand and manage traffic flow. The stability of traffic flow has been subjected to analytical studies using both linear and nonlinear analyses. These analyses are crucial for understanding the behavior of traffic flow and assessing its stability under various conditions. In order to analyze nonlinear behavior, we derive the mKdV equation to describe traffic behavior near critical points where interruptions are likely to occur. Moreover, increasing the control coefficient of the electronic throttle angle along with the interruption probability contributes to enhancing the stability of traffic flow. Also, the results from the numerical simulation demonstrate that incorporating both traffic interruption probability and throttle angle can effectively lessen and alleviate traffic congestion. These findings align remarkably well with the outcomes obtained from the analytical analyses. Thus, the findings demonstrate the potential of the proposed IP-ET model in improving the understanding and management of traffic flow in the context of connected and autonomous vehicles. Indeed, while the current study presents valuable insights into the impact of traffic interruption probability and throttle angle on traffic flow in a one-road system, there is significant potential for further advancements by extending the research to a road network setting.

VII. DECLARATION OF CONFLICTS INTEREST

The authors have not disclosed any conflicts of interest related to this work.

VIII. AUTHOR CONTRIBUTION STATEMENT

- **Sunita:** Modeling, analysis and simulation of the problem.
- **Poonam Redhu:** Guiding the planned work.
- The manuscript was written by Poonam Redhu and Sunita.

REFERENCES

[1] A. Talebpour and H. S. Mahmassani, "Influence of connected and autonomous vehicles on traffic flow stability and throughput," Transportation research part C: emerging technologies **71**, 143–163 (2016).

[2] W. Wang, M. Ma, S. Liang, J. Xiao, and N. Yuan, "Modeling and stability analysis of car-following behavior for connected vehicles by considering driver characteristic," Proceedings of the Institution of Mechanical Engineers, Part D: Journal of Automobile Engineering , 09544070221145478 (2023).

[3] R. Zhang, S. Masoud, and N. Masoud, "Impact of autonomous vehicles on the car-following behavior of human drivers," Journal of trans- portation engineering, Part A: Systems **149**, 04022152 (2023).

[4] S. Yadav and P. Redhu, "Driver's attention effect in car-following model with passing under v2v environment," Nonlinear Dynamics , 1–17 (2023).

[5] G. H. Peng and R. J. Cheng, "A new car-following model with the consideration of anticipation optimal velocity," Physica A: Statistical Mechanics and its Applications **392**, 3563–3569 (2013).

[6] Y. He, Q. Zhou, C. Wang, J. Li, B. Shuai, L. Lei, and H. Xu, "Microscopic modelling of car-following behaviour: Developments and future directions," International Journal of Automotive Manufacturing and Materials , 6–6 (2023).

[7] P. Redhu and A. K. Gupta, "Delayed-feedback control in a lattice hydrodynamic model," Communications in Nonlinear Science and Numerical Simulation **27**, 263–270 (2015).

[8] P. Redhu and A. K. Gupta, "Effect of forward looking sites on a multi-phase lattice hydrodynamic model," Physica A: Statistical Mechanics and its Applications **445**, 150–160 (2016).

[9] D. C. Gazis, R. Herman, and R. W. Rothery, "Nonlinear follow-the-leader models of traffic flow," Operations research 9, 545–567 (1961).

[10] M. Brackstone and M. McDonald, "Car-following: a historical review," Transportation Research Part F: Traffic Psychology and Behaviour **2**, 181–196 (1999).

[11] R. E. Wilson and J. A. Ward, "Car-following models: fifty years of linear stability analysis–a mathematical perspective," Transportation Planning and Technology **34**, 3–18 (2011).

[12] Y. Li and D. Sun, "Microscopic car-following model for the traffic flow: the state of the art," Journal of Control Theory and Applications **10**, 133–143 (2012).

[13] P. G. Gipps, "A behavioural car-following model for computer simulation," Transportation research part B: methodological **15**, 105–111 (1981).

[14] M. Bando, K. Hasebe, A. Nakayama, A. Shibata, and Y. Sugiyama, "Dynamical model of traffic congestion and numerical simulation," Physical review E **51**, 1035 (1995).

[15] S. Albeaik, A. Bayen, M. T. Chiri, X. Gong, A. Hayat, N. Kardous, A. Keimer, S. T. McQuade, B. Piccoli, and Y. You, "Limitations and improvements of the intelligent driver model (idm)," SIAM Journal on Applied Dynamical Systems **21**, 1862–1892 (2022).

[16] H. Hao, W. Ma, and H. Xu, "A fuzzy logic-based multi-agent car-following model," Transportation Research Part C: Emerging Technologies **69**, 477–496 (2016).

[17] Bharti, P. Redhu, and K. Kumar, "Short-term traffic flow prediction based on optimized deep learning neural network: Pso-bi-lstm," Physica A: Statistical Mechanics and its Applications, 129001 (2023).

[18] D. Helbing and B. Tilch, "Generalized force model of traffic dynamics," Physical review E **58**, 133 (1998).

[19] R. Jiang, Q. Wu, and Z. Zhu, "Full velocity difference model for a car-following theory," Physical Review E **64**, 017101 (2001).

[20] X. Li, Y. Zhou, and G. Peng, "Impact of interruption probability of the current optimal velocity on traffic stability for car-following model," International Journal of Modern Physics C **33**, 2250041 (2022).

[21] M. Ma, J. Xiao, S. Liang, and J. Hou, "An extended car-following model accounting for average optimal velocity difference and backward-looking effect based on the internet of vehicles environment," Modern Physics Letters B **36**, 2150562 (2022).

[22] A. Abdelhalim and M. Abbas, "A real-time safety-based optimal velocity model," IEEE Open Journal of Intelligent Transportation Systems **3**, 165–175 (2022).

[23] Y. Li, L. Zhang, S. Peeta, X. He, T. Zheng, and Y. Li, "A car-following model considering the effect of electronic throttle opening angle under connected environment," Nonlinear Dynamics **85**, 2115–2125 (2016).

[24] Y. Li, H. Zhao, T. Zheng, F. Sun, and H. Feng, "Non-lane-discipline-based car-following model incorporating the electronic throttle dynamics under connected environment," Nonlinear Dynamics **90**, 2345–2358 (2017).

[25] Q. Yanyan, W. Hao, and R. Bin, "Car-following model of connected and autonomous vehicles considering multiple feedbacks," Journal of Transportation Systems Engineering and Information Technology **18**, 48 (2018).

[26] Y. Sun, H. Ge, and R. Cheng, "A car-following model considering the effect of electronic throttle opening angle over the curved road," Physica A: Statistical Mechanics and its Applications **534**, 122377 (2019).

[27] C. Yan, H. Ge, and R. Cheng, "An extended car-following model by considering the optimal velocity difference and electronic throttle angle," Physica A: Statistical Mechanics and its Applications **535**, 122216 (2019).

[28] S. Li, R. Cheng, and H. Ge, "An improved car-following model considering electronic throttle dynamics and delayed velocity difference," Physica A: Statistical Mechanics and its Applications **558**, 125015 (2020).

[29] H. Ge, S. Li, and C. Yan, "An extended car-following model based on visual angle and electronic throttle effect," Mathematics **9**, 2879 (2021).

[30] C. Zhai, W. Wu, and Y. Xiao, "Cooperative car-following control with electronic throttle and perceived headway errors on gyroidal roads," Applied Mathematical Modelling **108**, 770–786 (2022).

[31] S. C. Wong, B. Leung, B. P. Loo, W. Hung, and H. K. Lo, "A qualitative assessment methodology for road safety policy strategies," Accident   Analysis & Prevention **36**, 281–293 (2004).

[32] S. Wong, N. N. Sze, and Y. C. Li, "Contributory factors to traffic crashes at signalized intersections in hong kong," Accident Analysis & Prevention **39**, 1107–1113 (2007).

[33] L. Telesca and M. Lovallo, "Analysis of the temporal properties in car accident time series," Physica A: Statistical Mechanics and its Applica-tions **387**, 3299–3304 (2008).

[34] T. Tang, H. J. Huang, and G. Xu, "A new macro model with consideration of the traffic interruption probability," Physica A: Statistical Mechanics and its Applications **387**, 6845–6856 (2008).

[35] G. H. Peng, H. D. He, and W. Z. Lu, "A new lattice model with the consideration of the traffic interruption probability for two-lane traffic flow," Nonlinear Dynamics **81**, 417–424 (2015).

[36] T. Tie Qiao, H. Hai Jun, S. Wong, and J. Rui, "A new car-following model with consideration of the traffic interruption probability," Chinese Physics B **18**, 975 (2009).

[37] G. H. Peng, "A new car-following model with driver's anticipation effect of traffic interruption probability," Chinese Physics B **29**, 084501 (2020).

[38] H. Ge, R. Cheng, and S. Dai, "Kdv and kink–antikink solitons in car-following models," Physica A: Statistical Mechanics and its Applications 357, 466–476 (2005